Spectral rigidity in scatterer-perturbed systems: the case of nonhydrogenic atoms in fields

LETTER TO THE EDITOR

Spectral rigidity in scatterer-perturbed systems: the case of nonhydrogenic atoms in fields

A Matzkin[1] and T S Monteiro[2]

[1] Laboratoire de Spectrométrie physique (CNRS Unité 5588), Université Joseph-Fourier
Grenoble-I, BP 87, 38402 Saint-Martin, France
[2] Department of Physics and Astronomy, University College London, Gower Street,
London WC1E 6BT, UK

Abstract
We investigate the influence of the atomic core on the spectral rigidity of the
spectrum of nonhydrogenic atoms in a magnetic field. Quantum calculations for
atoms with varying core properties are undertaken and the rigidity compared
to the hydrogenic one. We find that the presence of a scatterer does not
systematically induce chaos: in certain cases the nonhydrogenic spectrum is
less rigid than the scatterer-free hydrogenic one, whereas a chaotic system is
usually associated with more rigid spectra than regular systems. A semiclassical
theory based on the geometrical theory of diffraction is developed to understand
these findings, and the semiclassical calculations of the diffractive contribution
to the spectral rigidity agree with the quantum results.

PACS numbers: 03.65.Sq, 32.60.+i, 05.45.Mt

(Some figures in this article are in colour only in the electronic version)

It is well known that the level statistics of simple quantum systems are connected to the
dynamical behaviour of their classical counterparts. This connection is rendered manifest
by the use of semiclassical methods, whereby the level spectrum of a quantum system is
obtained in terms of classical periodic orbits by means of trace formulae. Berry [1] showed
how the spectral rigidity $\Delta(L)$, which measures deviations of the spectral staircase from a
straight line, could be obtained in the semiclassical limit in terms of classical quantities:
the mean properties of long orbits give rise to a universal behaviour for generic chaotic or
integrable systems, whereas the shortest orbits imprint a system specific signature. When a
scatterer is added to a system, the trace formula acquires additional terms (diffractive orbits)
produced by the diffraction of the semiclassical waves on the scatterer [2]. Lately interest has

focused on the influence of a scatterer on the statistics. For example, in chaotic systems a point-like scatterer does not modify the statistics, due to a cancellation of the universal part of the spectral form factor which was explained semiclassically in terms of the correlations between periodic-diffractive and diffractive orbits [3, 4]. On the other hand, perturbations in integrable or mixed phase space systems affect the statistics. Semiclassical methods allow us to determine long-range correlations (relative to the mean level spacing) such as the form factor provided diffraction is appropriately taken into account, as has recently been done for rectangular billiards [5].

We investigate here nonhydrogenic Rydberg atoms in a static magnetic field. The hydrogen atom in a magnetic field has been a paradigm of an experimentally accessible system displaying quantum chaos [6]. Nonhydrogenic Rydberg atoms, in which a scatterer—the atomic core—characterized by short-range phase shifts known as quantum defects is added to the hydrogenic problem have also been widely investigated. Much work has focused on how short-range statistics such as the nearest neighbour spacing (NNS) distributions are modified as a function of the quantum defect of the scatterer: irrespective of the phase space properties (near-integrable, mixed or chaotic), level repulsion was seen to increase with the core-scattering intensity. From these results emerged the idea of 'core-induced chaos' [7], though whether this chaos is of the same nature as generic chaos has been discussed [8]. It is therefore of interest to investigate long-range statistics, which are the only ones amenable to a semiclassical treatment and may as such shed new light on the chaotic nature of the diffractive process.

In the present work, we calculate the spectral rigidity for nonhydrogenic Rydberg atoms in a magnetic field determined from accurate quantum calculations, and compare it to the hydrogenic results, in the mixed phase space and near-integrable regimes. A surprising finding is that contrary to expectations based on 'core-induced chaos' arguments and to numerical results obtained on billiards [9], adding a scatterer does not necessarily yield a spectral signature characteristic of more chaotic dynamics than in the scatterer-free system. Indeed, we have observed in some cases less rigid spectra in nonhydrogenic atoms than in the hydrogenic case. To understand these results, we go beyond previous work [10], which focused on s-wave scattering in the integrable regime, and account for the difference between nonhydrogenic and hydrogenic rigidities by means of a semiclassical formalism based on the geometrical theory of diffraction, which allows us to obtain a trace formula for nonhydrogenic atoms. This trace formula will then be employed in the semiclassical expression of the spectral rigidity. We will see that for these systems, with a small but fixed value of $\hbar$, non-universal contributions to the diffractive spectral rigidity are particularly important. Employing an effective diagonal approximation to the form factor in the one-scatter approximation, we obtain semiclassical results in reasonable agreement with the quantum calculations.

As is known, the hydrogen atom in a magnetic field possesses axial symmetry reducing the semiclassical problem from three to two dimensions. It also has an important scaling property [6], which allows the calculation of quantum spectra while keeping the classical dynamics fixed. The classical dynamics of the electron does not depend separately on its energy E and the magnetic field strength γ but is invariant provided $\epsilon = E\gamma^{-2/3}$ is constant. ϵ is the scaled energy and the dynamics goes from the near-integrable to the chaotic regime as ϵ is varied. We will use scaled variables throughout: $\hbar$ is replaced by $\kappa^{-1} \equiv \gamma^{1/3}$ which plays the role of an effective Planck constant. For a given value of ϵ, the fluctuations in the density of states are given by the trace formula

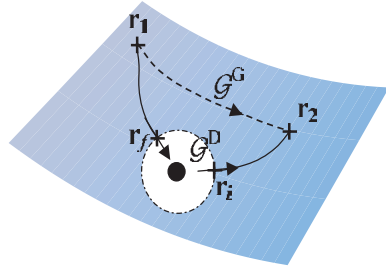$$d^G(\kappa) = \frac{1}{2\pi} \sum_p A_p^G \exp(i\kappa S_p) \tag{1}$$

Figure 1. $\mathcal{G}^G$ is carried by paths connecting r_1 directly to r_2, whereas $\mathcal{G}^D$ takes into account trajectories that hit the scatterer. The white circle around the scatterer is the inner zone, where a quantum treatment is appropriate.

where the sum runs on the periodic orbits p of the system and the G stands for 'geometric' (to distinguish these contributions from the diffractive ones). Complex conjugation will be implicitly understood. S_p is the action, and the amplitude is

$$A_p^G = \frac{S_p \exp(-\mathrm{i}(\alpha_p + \beta_p))\pi/2}{|\det(M_p - I)|^{1/2}} \tag{2}$$

where α is the Maslov index, β is related to the sign of the mixed derivatives of S transverse to the periodic orbit and M is the 2×2 monodromy matrix.

In nonhydrogenic Rydberg atoms, the presence of the core modifies the Green's function; in the semiclassical limit, this means that besides the geometrical classical path linking directly two points r and r', additional paths that hit the core must be taken into account (see figure 1). On the other hand, the scattering between the outer electron and the atomic core is intrinsically a quantum process and must be treated as such. To obtain the diffractive contribution to the trace formula, we proceed in the following steps that are sketched below; full details will be given elsewhere [11], in the more general context of multilevel quantum scatterers. Note that some of the arguments employed below are well known in the context of Closed Orbit theory which is a semiclassical treatment of photoabsorption for atoms in fields (see [12] and the references given in [13]).

First, we divide configuration space into two zones: a small inner zone around the core is divided from the outer zone (figure 1). In the inner zone the magnetic field is negligible and we have a simple Coulomb problem. Let $\mathcal{G}^G$ be the scatterer-free Green's function; the total Green's function is obtained by projecting the resolvent equation $\mathcal{G} = \mathcal{G}^G + \mathcal{G}^G T \mathcal{G}^G$, yielding

$$\mathcal{G}(r_2, r_1) = -16\pi \sum_{m, l \geqslant |m|} |m\rangle g_l^+(r_2) Y_{lm}(\theta_2) \sum_{m', l' \geqslant |m'|} \left[\delta_{ll'} f_{l'}(r_1) + T_{ll'} g_{l'}^+(r_1)\right] Y_{l'm'}^*(\theta_1)\langle m'| \tag{3}$$

where $r_2 > r_1$ and $Y_{lm}(\theta_i)$ stands for the spherical harmonic $Y_{lm}(\theta_i, 0)$. f_l and g_l are standing Coulomb waves respectively regular and irregular at the origin, and $g_l^\pm = (g_l \pm \mathrm{i} f_l)$ are outgoing and incoming Coulomb waves. The T-matrix elements arise from the short-range core–electron interaction; we assume, as is often realized in atoms, that the T-matrix is diagonal and given by $T_l = (1 - \exp(2\mathrm{i}\pi\mu_l))/2\mathrm{i}$, where μ_l is the quantum defect for the lth partial wave. In the outer region, the excited electron is subjected to both the Coulomb and magnetic fields and a semiclassical approximation to the two-dimensional Green's function is appropriate. m, quantized along the magnetic field axis, is conserved, and for a given m the Green's function is given by the usual expression

$$\mathcal{G}_{sc}^G(r', r) = \sum_p (\hbar\sqrt{2\pi\hbar})^{-1} |\mathcal{D}_p|^{1/2} \exp(\mathrm{i}(S_p(r', r) - \alpha_p \pi/2 - 3\pi/4)) \tag{4}$$

where the sum runs on the classical trajectories connecting r and r'; we will denote by $\mathcal{G}^G_{sc(p)}$ the pth term of this sum. $\mathcal{D}_p$ is the standard determinant.

The second step is to connect the inner and the outer zones. To do so we consider $\psi(r_2)$, the wavefunction at r_2 produced by a unit source placed at r_1 that has scattered on the core, entering the inner region at r_f and leaving it at r_i (see figure 1). Then the wave arriving at r_f is simply $\mathcal{G}^G_{sc}(r_f, r_1)$. On the other hand, the most general solution in the inner zone is obtained from the Lippmann–Schwinger counterpart of equation (3) as

$$\sum_{l \geqslant |m|} c_{lm} Y_{lm}(\theta) \left[f_l(r_0) - \frac{i}{2}(\exp(2i\pi \mu_l) - 1) g_l^+(r_0) \right]. \tag{5}$$

The coefficients c_{lm} are obtained by matching at $r_f = (r_0, \theta_f)$ the *incoming* part of equation (5) to $\mathcal{G}^G_{sc}(r_f, r_1)$ in the stationary phase approximation (along the angle of stationary phase θ_{fp} for each trajectory p). The scattered outgoing wave in the inner zone is given by the *outgoing* part of equation (5), which leaves the inner zone at $r_i = (r_0, \theta_i)$. From the knowledge of the wavefunction on r_0, we can propagate the wavefunction semiclassically beyond r_0 as prescribed by Maslov [17],

$$\psi(r) = \sum_q \sqrt{\rho_q(r)} \exp(i(S_q - \alpha_q \pi/2 - 3\pi/4)) \tag{6}$$

where $\rho_q(r)$ is the solution of the transport equation for the density and is proportional to $\mathcal{D}_q$; q denotes the classical trajectories having left the boundary circle at $r_{iq} = (r_0, \theta_{iq})$. Employing the asymptotic expansion for $g_l^+(r_0)$ we rearrange terms so that the action propagates from and to the origin $r = 0$ and finally obtain $\psi(r_2)$ or equivalently the Green's function corresponding to the diffractive process as

$$\mathcal{G}^D(r_2, r_1) = |m\rangle\langle m| \sum_{q,p} \mathcal{G}^G_{sc(q)}(r_2, 0) C_{qp}(\mu; m) \mathcal{G}^G_{sc(p)}(0, r_1). \tag{7}$$

As in other works based on the geometrical theory of diffraction (e.g. [2, 15]), the diffractive Green's function is obtained from the free Green's function linked by a diffraction constant C_{qp} which is here given by

$$C_{qp}(\mu; m) = \sum_l i\hbar_{\text{eff}}^2 2^3 \pi^2 r_0 \sin\theta_{iq} \sin\theta_{fp} Y_{lm}(\theta_{iq}) Y_{lm}^*(\theta_{fp})(1 - \exp(2i\pi \mu_l)). \tag{8}$$

We have emphasized the dependence of C on the properties of the classical trajectories q and p and on the quantum property of the scatterer. $\hbar_{\text{eff}}$ is the mean value of κ^{-1}.

The third step consists in taking the trace of $\mathcal{G}^D$. This is done by using a stationary phase integration along the coordinates perpendicular to the orbit as detailed in [15]. The trace is then obtained as a sum over periodic orbits *closed at the origin* where for each orbit free geometric propagation $\mathcal{G}^G_{sc(q)}(0, 0)$ is weighted by the diffraction constant $C_{qq}(\mu; m)$. The diffractive density of states can be put in a form similar to equation (1),

$$d^D(\kappa) = \frac{1}{2\pi} \sum_q A_q^D \exp(i\kappa S_q) \tag{9}$$

with the diffractive amplitude

$$A_q^D = -i \sum_l \hbar_{\text{eff}}^{1/2} S_q \exp(-i(\alpha_q \pi/2 + 3\pi/4))(\exp(2i\pi \mu_l) - 1)$$

$$\times Y_{lm}(\theta_{iq}) Y_{lm}^*(\theta_{fq}) 2^{3/2} \pi^{3/2} \left| \frac{\sin\theta_{iq} \sin\theta_{fq}}{m_{12(q)}} \right|^{1/2} \tag{10}$$

where m_{12} is the element of M with the initial deviation in the momentum coordinate. Note that an expression equivalent to equation (10) in the particular case of s-wave scattering was inferred in [14] from the comparison of Fourier-transformed spectra of hydrogen and lithium atoms.

The spectral rigidity $\Delta(L)$ is defined as the least squares deviation of the staircase function $\mathcal{N}$ of the unfolded spectrum from a straight line, over a level range L. The semiclassical approximation to $\Delta(L)$ was derived in [1]; in scaled coordinates this can be put as

$$\Delta^{XY}(L) = \frac{1}{2\pi^2} \int_0^\infty \frac{\mathrm{d}\nu}{\nu} \frac{K^{XY}(\nu/\pi L)}{\nu/\pi L} \gamma(\nu) \tag{11}$$

with $\nu = LS/2\chi$, where $\chi \equiv \partial \langle \mathcal{N} \rangle / \partial \kappa$ is a constant due to scaling. $\gamma(\nu) = 1 - F^2(\nu) - 3[F'(\nu)]^2$ is known as the 'orbit selection function', where $F(\nu) \equiv \sin \nu / \nu$. K^{XY} is the spectral form factor, given by

$$K^{XY}(\sigma) \simeq \frac{1}{2\pi \chi} \left\langle \sum_{p,q} A_p^X [A_q^Y]^* \exp[\mathrm{i}(S_p - S_q)\kappa_0] \delta\left(S - \frac{S_p + S_q}{2}\right) \right\rangle \tag{12}$$

with $\sigma = \nu/\pi L = S/2\pi \chi$. The bracket denotes an average over the starting points κ_0. The indices X and Y are insignificant in the scatterer-free system. But in the nonhydrogenic case, the total density is given by $d = d^G + d^D$ and by following Berry's original derivation it is easily seen that the spectral rigidity takes the form $\Delta(L) = \Delta^{GG}(L) + \Delta^{GD}(L) + \Delta^{DD}(L)$ with each term being given by equation (11), and X and Y are obviously seen to refer to G or D contributions. Since Δ^{GG} is the rigidity for the scatterer free system, the influence of diffraction on the spectral rigidity—which is the quantity of interest in the present work—is given by

$$\Delta_{\mathrm{diff}}(L) = \Delta^{GD}(L) + \Delta^{DD}(L) = \Delta(L) - \Delta^{GG}(L). \tag{13}$$

To determine Δ^{GD} and Δ^{DD}, we use two different approximations for the form factor which have been discussed in [1]. For very short orbits ($\sigma < \sigma^*$, with $\sigma^* \ll 1$), the diagonal approximation involves keeping only the contributions of orbits having the same action. Discarding accidental orbit degeneracies, we sum on the sole short orbits closed at the origin, which are both solutions of the geometric and of the diffractive systems (with different amplitudes however) and obtain

$$\Delta^{XY}(L) = \sum_{q \in \{\sigma_q < \sigma^*\}} \frac{1}{2\pi^2} \frac{1}{S_q^2} A_q^X [A_q^Y]^* G\left(\frac{LS_k}{2\chi}\right). \tag{14}$$

To take into account longer orbits, up to the Heisenberg 'time' $\sigma_h = 1$, it is necessary to invoke classical sum rules. For the term $\Delta^{DD}(L)$, the relevant sum rule for transient orbits has been given by Sieber [16]. We use average angles $\bar{\theta} = \pi/4$ and write the sum $\sum_q |m_{12(q)}|^{-1} \delta(S - S_k^j) \approx 2\pi \Sigma(\epsilon)^{-1}$ to obtain

$$K^{DD}(1 > \sigma > \sigma^*) \approx \frac{1}{2\pi \chi} \hbar_{\mathrm{eff}} 2^5 \pi^4 \sum_l \frac{1}{\Sigma(\epsilon)} \sin^2 \pi \mu_l |Y_{lm}(\bar{\theta})|^4 S^2 \tag{15}$$

where $\Sigma(\epsilon)$ is the volume of the energy surface in the scaled phase space at scaled energy ϵ. The term $\Delta^{GD}(L)$ involves cross correlations between diffractive and geometric orbits. Relevant sum rules have been given in [3, 4]; they rely on expanding $S_p - S_q$ in terms of $|\det(M - I)|$ and $|m_{12}|$. Integration along the boundary circle (perpendicular to the orbits) yields

$$K^{GD}(1 > \sigma > \sigma^*) \approx \frac{-1}{2\pi \chi} \hbar_{\mathrm{eff}} \frac{2^{5/2} \pi^3}{\sqrt{2 + \sqrt{2}}} \sum_l \frac{1}{\Sigma(\epsilon)} (1 - \exp(2\mathrm{i}\pi \mu_l)) |Y_{lm}(\bar{\theta})|^2 S^2 \tag{16}$$
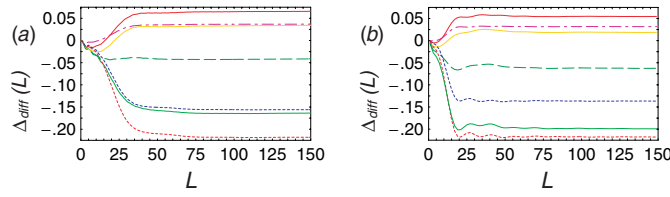
Figure 2. (*a*) Difference of spectral rigidities $\Delta(L; \mu) - \Delta(L; \mu = 0)$ between nonhydrogenic and hydrogen atoms obtained from quantum calculations at $\epsilon = -0.3, m = 1$. The different curves correspond from top to bottom to $\mu = 0.15$ (red solid), $\mu = 0.05$ (purple dot-dashed), $\mu = 0.25$ (yellow solid), $\mu = 0.35$ (green dashed), $\mu = -0.15$ (blue dotted), $\mu = 0.5$ (green solid) and $\mu = -0.25$ (red dotted). (*b*) Semiclassical results for the diffractive contribution to the spectral rigidity $\Delta_{\text{diff}}(L)$ for nonhydrogenic atoms with varying μ.

where we have again used the approximation $\bar{\theta} = \pi/4$. Lastly, orbits beyond σ_h enter the form factor through a semiclassical sum rule which ensures that these long orbits generate the mean level density [1]. But adding a scatterer does not change the mean level density, so these orbits cannot enter the determination of $\Delta_{\text{diff}}(L)$; in other words we assume (without any other proof than this heuristic argument) that the contributions $K^{DD}(\sigma \gg 1)$ and $K^{GD}(\sigma \gg 1)$ cancel each other so that the contributions for $\sigma \gg 1$ on the right-hand side of equation (13) vanish.

We have thus determined, within the approximations involved and for $L \gg 1$, the influence of diffraction on the rigidity. Equation (14) with A_q^X and A_q^Y replaced by the relevant expressions (2) or (10) gives non-universal (NU) terms; note that in the one-scatter approximation, Δ_{NU}^{GD} is proportional to $\hbar_{\text{eff}}^{1/2}$ and Δ_{nu}^{DD} to $\hbar_{\text{eff}}$. On the other hand, the universal terms obtained by replacing equations (15) and (16) in equation (11) do not depend on $\hbar_{\text{eff}}$ (since the integral is seen to be $2\pi\chi \int_{\sigma^*}^1 d\sigma\,\gamma(\pi L\sigma)$, which scales as $\hbar_{\text{eff}}^{-1}$). Still, for finite $\hbar_{\text{eff}}$ and large L, NU terms can be important, whereas K^{DD} and K^{GD} tend to cancel each other, a property arising from the unitarity of the T-matrix, $\text{Im}\,T_l = -|T_l|^2$ (the approximations made here do not allow exact cancellation to occur). Note, however, that in the more general case of a multilevel scatterer, for which the unitarity equations involve the non-diagonal elements, NU and universal contributions can both compete [11].

We have calculated quantum mechanically the energy levels for hydrogen and for nonhydrogenic atoms with a single quantum defect μ in the $l = 1$ partial wave, for $m = 1$ at $\epsilon = -0.3$ (mixed phase space) in the range $\kappa = 60$–120 (encompassing about 3500 levels). χ was determined by fitting the spectral staircase to a second-order polynomial in κ. The rigidities for hydrogen $\Delta(L; \mu = 0)$ and for a nonhydrogenic atom with a given quantum defect $\Delta(L; \mu)$ were calculated, and the influence of the scatterer in the statistics obtained from the quantum spectra is put in evidence by the difference $\Delta(L; \mu) - \Delta(L; \mu = 0)$. This is precisely the quantity to be compared to the diffractive contribution to the rigidity obtained semiclassically above, equation (13), for which we calculated the relevant classical quantities. The quantum results are shown in figure 2(*a*) for several values of μ. The most striking feature is that for a certain number of μ values, Δ_{diff} is positive. This means that the spectrum of the corresponding nonhydrogenic atom is *less rigid* than the spectrum of hydrogen, whereas it could be expected that the increase in correlations induced by the scatterer would systematically result in more disordered dynamics, associated with a stiffer spectrum.

Figure 2(*b*) shows our semiclassical results. The main behaviour obtained from the quantum spectra is well reproduced, in particular the sign of $\Delta_{\text{diff}}(L)$ which determines whether the influence of diffraction yields a rigidity higher or lower than in the scatterer-free case.
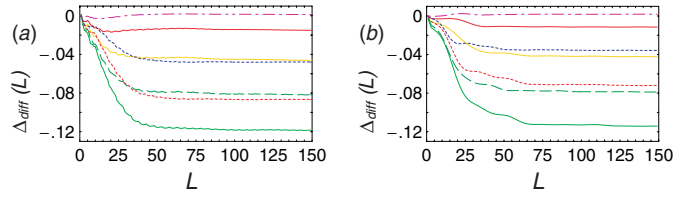
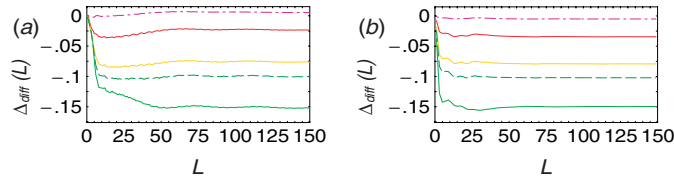**Figure 3.** Same as figure 2 but for $\epsilon = -0.3$, $m = 0$.

Figure 4. Same as figure 2 but for $\epsilon = -0.8$, $m = 1$.

Note that the semiclassical results were multiplied by a global factor ~ 1.1; this global rescaling presents one of the main limitations of the present treatment and is due to the sensitivity arising from the choice of σ^* in equation (14). Generic chaotic systems displaying exponentially decreasing amplitudes would display little sensitivity to the value of σ^*, but this is not true in mixed phase space. For the sake of comparison, we have also plotted the quantum and semiclassical results for the same system but with $m = 0$ (figure 3), whereas figure 4 displays similar results in the near-integrable regime ($\epsilon = -0.8$, $\kappa = 80$–150 containing about 1500 levels).

The present results show that the diffractive contributions to the rigidity are dominated by the shortest periodic and diffractive orbits. The semiclassical formalism developed above can further allow us, in simple cases, to pinpoint the cause of the observed rigidity. Indeed, a single typical orbit (with initial and final angles in the first quadrant) contributes to the sign of Δ^{GD} in equation (14) as $1 - \cos 2\pi\mu \pm \sin 2\pi\mu$ (depending on the additional phase β of equation (2)), which is negative except in one of the intervals $[0, \pm 0.25]$ where it becomes slightly positive. When many orbits with similar amplitudes are included, we may expect on average Δ^{GD} to be proportional to $\cos 2\pi\mu - 1 < 0$. However, the situation in which a few orbits have large geometric and diffractive amplitudes interfering in a constructive way cannot be discarded. This is precisely the situation portrayed in figure 2: the second and the fourth return of the orbit perpendicular to the field, which is stable, have very large amplitudes, due to a near-rational winding number arising from a bifurcation at a slightly lower scaled energy. Jumps in Δ_{NU} are indeed observed when these orbits are included in the sum (14). Note that when $m = 0$ perpendicular orbits do not contribute to Δ_{diff}, as A^D given by equation (10) vanishes when $l = 1$. The diffractive rigidity has then indeed a very different behaviour, as is seen in figure 3.

Deviations from universality in the rigidity of non-diffractive systems were observed before [18], and generally attributed to peculiar families of orbits. In the case of diffractive systems the general trend, as observed, for example, in integrable billiards [9], is that the spectrum becomes less rigid as the intensity of the added scatterer is increased. However, we have seen here that the rigidity has no simple dependence on the intensity of the scatterer, $|\mu|$, as the complex value of the T-matrix is important. In fact, the diffractive contribution depends in a crucial way on the classical properties of the shortest orbits that hit the scatterer.

Some of these orbits may therefore affect the rigidity in a particular way, yielding long-range statistics that would incorrectly appear to reflect a scatterer-perturbed system displaying more ordered dynamics than the scatterer-free system. In contrast, we have determined the NNS distributions of the spectra calculated above and in all cases, level repulsion was seen to depend on $|\mu|$, level repulsion increasing with $|\mu|$. Similar results were recently observed in circular billiards [19], where for intense perturbations the NNS moved from a Poisson to a semi-Poisson distribution, though the form factor did not correspond to the semi-Poisson result. All these findings purport the view that generic and scatter-induced chaos do not follow the same pattern.

References

[1] Berry M V 1985 *Proc. R. Soc.* A **400** 229
[2] Vattay G, Wirzba A and Rosenqvist P E 1994 *Phys. Rev. Lett.* **73** 2304
[3] Sieber M 2000 *J. Phys. A: Math. Gen.* **33** 6263
[4] Bogomolny E, Leboeuf P and Schmit C 2000 *Phys. Rev. Lett.* **85** 2486
[5] Rahav S and Fishman S 2002 *Phys. Rev.* E **65** 067204
[6] Friedrich H and Wintgen D 1989 *Phys. Rep.* **183** 37
[7] Jans W, Monteiro T S, Schweizer W and Dando P A 1993 *J. Phys. A: Math. Gen.* **33** 1247
     Courtney M and Kleppner D 1996 *Phys. Rev.* A **53** 178
[8] Jonckheere T, Grémaud B and Delande D 1998 *Phys. Rev. Lett.* **81** 2442
     Held H and Schweizer W 2000 *Phys. Rev. Lett.* **84** 1160
[9] Cheon T and Shigehara T 1996 *Phys. Rev.* E **54** 3300
     Shigehara T, Mizoguchi H, Mishima T and Cheon T 2001 *Nonlinear Anal.* **47** 3555
[10] Walker P N and Monteiro T S 2000 *Phys. Rev.* E **61** 6444
[11] Matzkin A and Monteiro T S in prepraration
[12] Du M L and Delos J B 1988 *Phys. Rev.* A **38** 1913
[13] Matzkin A, Dando P A and Monteiro T S 2002 *Phys. Rev.* A **66** 013410
[14] Dando P A, Monteiro T S and Owen S M 1998 *Phys. Rev. Lett.* **80** 2797
[15] Bruus H and Whelan N D 1996 *Nonlinearity* **9** 1023
[16] Sieber M 1999 *J. Phys. A: Math. Gen.* **32** 7679
[17] Maslov V P and Fedoriuk M V 1981 *Semi-Classical Approximation in Quantum Mechanics* (Dordrecht: Reidel)
[18] Hönig A and Wintgen D 1989 *Phys. Rev.* A **39** 5642
     Sieber M, Smilansky U, Creagh S C and Littlejohn R G 1993 *J. Phys. A: Math. Gen.* **26** 6217
[19] Rahav S, Richman O and Fishman S 2003 *J. Phys. A: Math. Gen.* **36** L529